The clonal structure and dynamics of the human T cell response to an organic chemical hapten.

1 **Tahel Ronel[1], Matthew Harries[2,3], Kate Wicks[2], Theres Oakes[1], Helen Singleton[2], Rebecca**
2 **Dearman[2], Gavin Maxwell[4] and Benny Chain[1,5*]**

3 [1]Division of Infection and Immunity, University College London, London, United Kingdom

4 [2]Faculty of Biology, Medicine and Health, University of Manchester, Manchester, United Kingdom

5 [3]Salford Royal NHS Foundation Trust (Dermatology Centre), Salford, UK

6 [4]Safety and Environmental Assurance Centre, Unilever, Colworth Science Park, Bedford, United
7 Kingdom

8 [5]Department of Computer Science, University College London, London, United Kingdom

9 *** Correspondence:**
10 Professor Benny Chain
11 b.chain@ucl.ac.uk

Abstract

15 Diphenylcyclopropenone (DPC) is an organic chemical hapten which induces allergic contact
16 dermatitis, and is used in treatment of warts, melanoma and alopecia areata. This therapeutic
17 setting therefore provided an opportunity to study T cell receptor (TCR) repertoire changes in
18 response to hapten sensitization in humans. Repeated exposure to DPC induced highly dynamic
19 transient expansions of a polyclonal diverse T cell population. The number of TCRs expanded early
20 after sensitization varies between individuals, and predicts the magnitude of the allergic reaction.
21 The expanded TCRs show preferential TCR V and J gene usage, and consist of clusters of TCRs
22 with similar sequences, two characteristic features of antigen-driven responses. The expanded
23 TCRs share subtle sequence motifs that can be captured using a Dynamic Bayesian Network.
24 These observations suggest the response to DPC is mediated by a polyclonal population of T cells
25 recognizing a small number of dominant antigens.

26

Introduction

Diphenylcyclopropenone (DPC) is an example of a hapten, a small organic compound that reacts with biological macromolecules including proteins to form immunogenic conjugates. It is a potent skin sensitizer (Mose et al., 2017a; Stute, Hausen, & Schulz, 1981) and, since it is non-mutagenic in the AMES assay (Wilkerson et al., 1987), it has been used as an immunostimulant in the treatment of warts (Buckley et al., 1999), melanoma (Read et al., 2017) and alopecia (Ashworth et al., 1989; Karanovic et al., 2018; Lee et al., 2018). DPC can also act as an adjuvant to conventional immunization (Moos et al., 2012). Because of its clinical applications, and because it is not commonly found in the environment, DPC serves as an interesting model to study primary and secondary responses to chemical haptens in humans, although the confounding effects of any underlying clinical condition in the treated individuals must obviously be considered. Clinically, repeated exposure results in rapid sensitization, but the magnitude of the resulting allergic contact dermatitis (ACD) does not continue to increase during repeated exposure (Mose et al., 2017a), suggesting the existence of regulatory processes. Global expression profiling at the site of elicitation suggested a predominantly Th1/Th17 type T cell infiltration, whose dynamics mirrored the clinical and histopathological picture (Mose et al., 2017b). High serum interleukin-4 (IL4) and low interleukin-12 (IL12) were observed in patients with alopecia showing a favorable response to DPC treatment.

As part of an extended project to understand more fully the immunological events leading to ACD, and hence generate better tools for chemical risk assessment (Kimber et al., 2012), we have measured the T cell receptor repertoire (TCRrep) changes in ex vivo blood samples collected from patients before and after therapeutic sensitization with DPC. In a previous study, we used a newly developed quantitative, robust experimental and computational pipeline (Oakes et al., 2017a) to measure changes in the TCRrep following in vitro re-stimulation of blood from individuals allergic to the environmental contact allergen paraphenylene diamine (Oakes et al., 2017b). A limitation of the study was that the extent of allergen exposure prior to challenge was unknown. Here we extend these studies to document in vivo changes to the TCRrep during primary and secondary sensitization with DPC in a small cohort of patients with alopecia. Exposure to DPC results in transient expansions of a set of related TCR sequences in the peripheral blood. The number of responding TCRs correlates with the extent of sensitization, and is not observed in unexposed individuals. The results suggest that exposure to a contact allergen in vivo stimulates an initial polyclonal expansion of antigen-specific responding T cells which, however, does not increase on further repeated exposure to antigen.

Results

We carried out TCRseq on unfractionated blood samples from 29 patients with alopecia (**Table 1**).

_____

Table 1: Demographics of the study population.

ID	Age	Sex[1]	Alopecia[2]	TCRseq sets[3]	Flow cytometry[4]	Patch test scores[5]
1	50-59	F	AA (>50%)	0		✓
2	10-19	M	AU	0		✓
3	20-29	F	AT	3		✓
4	50-59	F	AT	4	✓	✓
5	50-59	M	AA (>50%)	3	✓	✓
6	40-49	M	AA (>50)	4	✓	✓

	Age	Sex[1]	Type[2]	[3]	[4]	[5]
7	40-49	M	AU	4	✓	✓
8	30-39	F	AA (>50%)	3		✓
9	30-39	F	AT	0	✓	✓
10	20-39	F	AT	1	✓	
11	30-39	M	AU	1		
12	20-29	F	AA (>50%)	0	✓	✓
13	30-39	F	AT	1	✓	
14	30-39	F	AA (<50%)	3		✓
15	40-49	F	AU	4	✓	✓
16	40-49	F	AA (<50%)	4	✓	✓
17	50-59	F	AT	3		✓
18	20-29	F	AT	1		
19	50-59	F	AU	2		
20	50-59	F	AU	4		✓
21	10-19	M	AA (>50%)	3		✓
22	30-39	F	AA (>50%)	4		✓
23	50-59	F	AU	4		✓
24	40-49	F	AA (<50%)	4		✓
25	40-49	F	AT	3		✓
26	60-69	F	AA (<50%)	2		
27	30-39	F	AA (>50%)	1		
28	30-39	M	AA (<50%)	3		✓
29	50-59	F	AT	4		✓
30	60-69	F	AT	3		✓
31	30-39	F	AA (>50%)	1		
32	20-29	F	AA (<50%)	0		✓
33	40-49	F	AU	3		
34	40-49	F	AA (>50%)	3		

[1]F: female; M: male; [2]AA: alopecia areata (<50% or >50% scalp involvement); AT: alopecia totalis; AU: alopecia universalis. [3]The number of time points for which TCRseq data was obtained. [4]Indicates the patients for whom PBMC flow cytometry data were available. [5]The patients for whom patch test scores were available.


Samples were collected before (referred to as the pre-sensitization (PS) sample, Week 0, n=25 samples) and at one to three time points after sensitization with DPC (**Figure 1A**), taken at two weeks (PT1, n=23), six weeks (PT2, n=18) and approximately 24 weeks (PT3, n=17) post-sensitization. As controls, we carried out TCRseq on five healthy volunteers, for which we had time points that matched the 0, 2 and 6-week time points of the DPC sensitized group. We obtained a total of 24,431,855 distinct TCR sequences, of which 17,451,853 were unique across all samples. The number of TCR sequences obtained varied between samples (mainly due to small differences in volume of individual libraries when preparing the pooled library for sequencing) and are shown in **Supplementary File 1**. The median number of TCRs per sample was 95,638 (range 23,224-

77　690,600) and the median number of unique TCRs per sample was 75,111 (range 19,095-342,336).
78　Analyses included every patient for whom the relevant time points (and patch test data where
79　relevant) were available, and this number is indicated in the respective figure legends.

80　**Repeated exposure to DPC does not alter the global structure of the peripheral blood TCR**
81　**repertoire.**

82　The major T cell sub-populations (CD4/CD8, naive, central memory, effector memory and effector
83　memory RA revertant (Fletcher et al., 2005)) were quantified by flow cytometry and did not change
84　significantly after exposure to DPC (**Figure 1B**, two-sided paired t-tests corrected for multiple
85　testing, p=0.48, p=0.74, p=0.49, and p=0.74 for CD4, and **Figure 1C,** p=0.11, p=0.72, p=0.72 and
86　p=0.37 for CD8 naive, central, effector and effector memory RA revertant cells respectively).
87　Similarly, TCR repertoire diversity, captured by the Shannon diversity index, or the clonal expansion
88　captured by the Gini inequality coefficient, did not differ significantly before and after exposure to
89　DPC (**Figure 1D,E**, Kruskal-Wallis rank sum tests, p=0.89 and p=0.90 respectively), nor between
90　the different time points post-sensitization (**Figure 1G,H**, Kruskal-Wallis rank sum tests, p=0.96 and
91　p=0.95 respectively). Finally, the number of TCRs found at frequencies above 1 in 1000, which
92　correspond to the most abundant 6% of the repertoire on average, did not change as a result of
93　sensitization (**Figure 1F,I**, Kruskal-Wallis rank sum tests, p=0.12 and p=0.91 respectively). The
94　corresponding analyses for the alpha chain sequences are shown in **Supplementary File 2.**. There
95　was therefore no evidence that exposure to DPC, a potent skin sensitizer, caused global alterations
96　in the structure of the TCR repertoire.
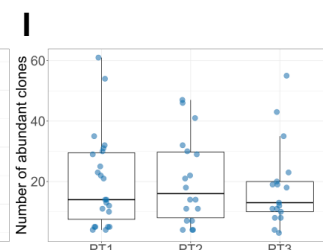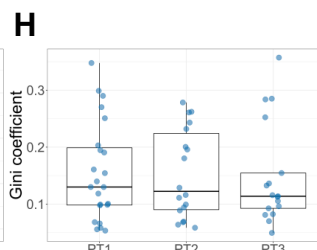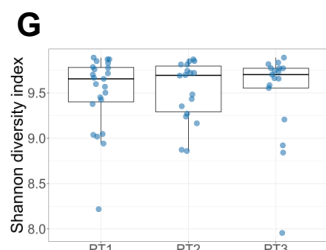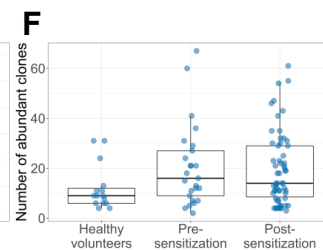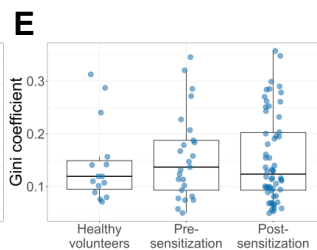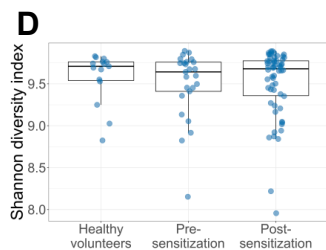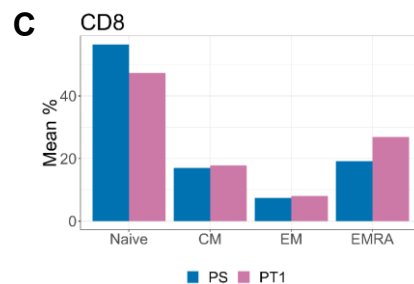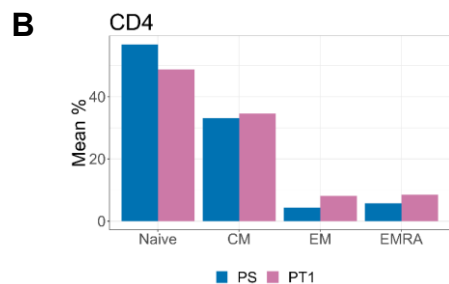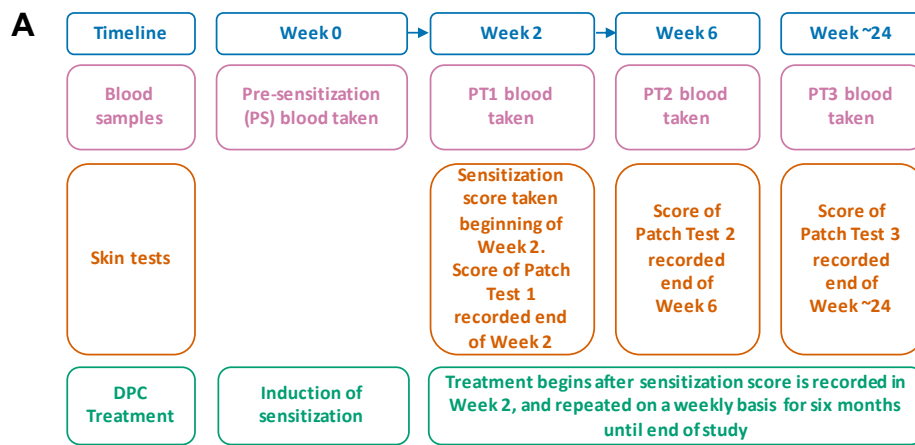
Figure 1: Repeated exposure to DPC does not alter the global structure of the peripheral blood TCR repertoire.

(A) The study outline, showing when bloods were drawn, skin tests were performed and DPC treatment was applied during the ~24 weeks of participation in the study. The four timepoints at which sensitization scores were recorded and blood samples were taken are referred to throughout the paper as PS (pre-sensitization, Week 0), PT1 (Patch Test 1, Week 2), PT2 (Patch Test 2, Week 6) and PT3 (Patch Test 3, around Week 24). In all cases bloods were drawn prior to application of the patch test. **(B)-(C)** The PS and PT1 blood samples of ten patients were analyzed using flow cytometry. The mean percentage of total naive, central memory (CM), effector memory (EM) and effector memory RA expressing (EMRA) cells in the (B) CD4 and (C) CD8 compartments are shown. Paired t-tests with Benjamini-Hochberg correction for multiple testing were performed to check for significant differences between the pre- and post-sensitization cell number distributions for each subpopulation. All p-values were considerably higher than the 0.05 significance threshold. **(D)** The

110 Shannon diversity index of the healthy volunteers (n=15 samples from five individuals), pre-sensitization
111 (n=25) and post-sensitization (n=58; from all three time points) TCR repertoire samples. All samples were
112 randomly subsampled to the minimum sample size (21,838 beta TCRs), and the Shannon diversity index of
113 the subsample was then calculated. Each sample is represented by a dot. The box plots show the median,
114 and lower and upper quartiles of each group. Differences in the distribution of the three groups were tested
115 using Kruskal-Wallis rank sum test and were non-significant (p=0.87). **(E)** The Gini inequality coefficient of the
116 healthy volunteers, pre-sensitization and post-sensitization TCR repertoire samples, subsampled as in (D).
117 Differences in the distribution of the three groups were tested using a Kruskal-Wallis rank sum test and were
118 non-significant (p=0.89). **(F)** The number of TCRs that appear with frequency of 1/1000 or higher in each
119 sample (termed 'abundant TCRs'), for the healthy volunteers, pre-sensitization and post-sensitization samples,
120 subsampled as in (D) and (E). A Kruskal-Wallis rank sum test revealed no statistical difference between the
121 groups (p=0.14). **(G)-(I)** Sensitized samples were separated according to time point: PT1 (n=23), PT2 (n=18)
122 and PT3 (n=17). The Shannon diversity index (G), the Gini coefficient (H) and the number of abundant clones
123 (I) of these subsamples were then calculated. Kruskal-Wallis rank sum tests were used to compare between
124 the three groups in each case. All tests showed no statistically significant difference, with p-values p=0.97,
125 p=0.96 and p=0.90 respectively.

126 _____
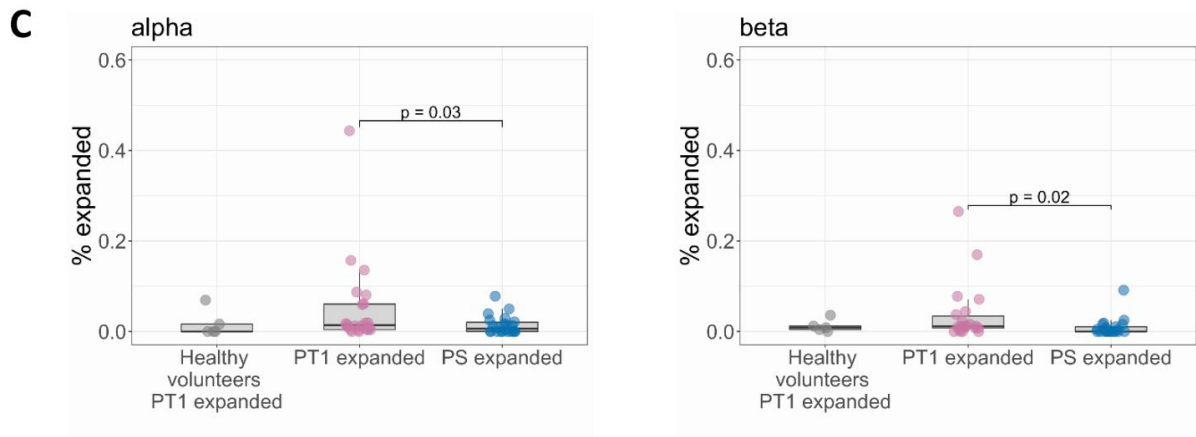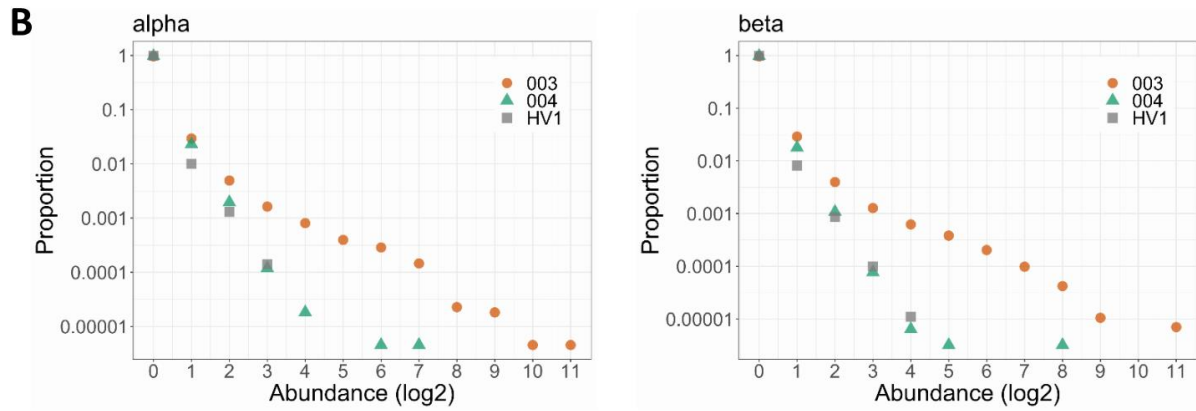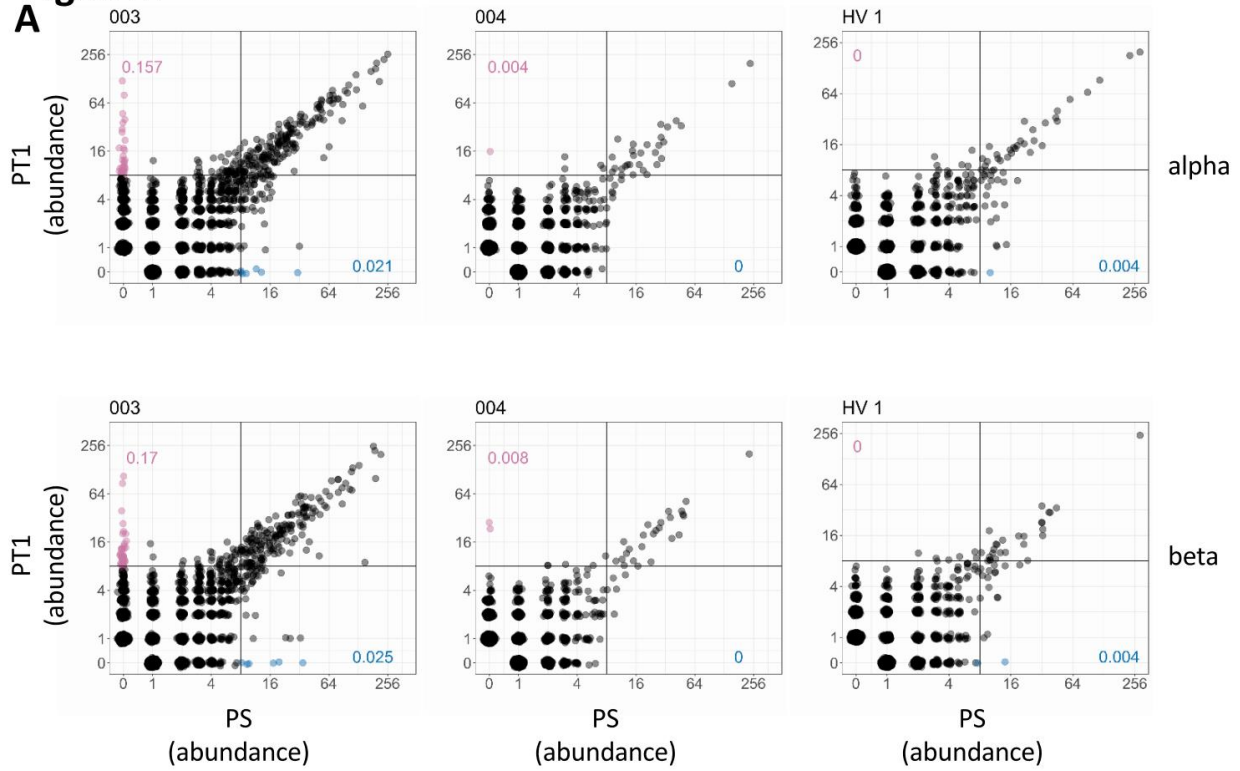
127 Sensitization with DPC induces a transient expansion in the frequency of a small subset of
128 the TCR repertoire.

129 We next looked for evidence of changes in individual TCR sequences following exposure to DPC.
130 We plotted the abundance of each TCR before sensitization and after sensitization (at PT1)
131 (representative examples are in **Figure 2A**; all individuals in **Supplementary File 3)**. We observed
132 that, in a number of individuals, there was a population of TCRs which were absent before
133 sensitization and present at relatively high abundance after sensitization (indicated by the pink dots
134 in the left panels of **Figure 2A**). This change is seen clearly in the abundance profile of all TCRs that
135 were absent in the pre-sensitization sample, but present after sensitization **(Figure 2B)**. On the
136 basis of these profiles, we counted the proportion of TCRs absent at PS and present at PT1 with an
137 abundance of 8 times or above. The remainder of this study focuses on this population, which we
138 refer to as PT1 expanded. The percentages of PT1 TCRs which are expanded in each individual are
139 summarized for patients and healthy volunteers in **Figure 2C.** For comparison, we calculated the
140 percentage of TCRs absent at PT1 but present at PS with an abundance of 8 times or above
141 (referred to as PS expanded). The range of percentages of expanded TCRs at PT1 is clearly much
142 greater in the patients than in the healthy volunteers (between 0 to 2 weeks), although the medians
143 are not significantly different (p=0.16, and p=0.47 for alpha and beta respectively, Mann-Whitney).
144 The percentage of expanded TCRs at PT1 in the patients is significantly larger than the percentage
145 of TCRs which were expanded at PS and absent at PT1 (p=0.02 for alpha, p=0.03 for beta, paired
146 Mann-Whitney). This is not the case for the healthy volunteers (p=0.79 for alpha, p=0.59 for beta,
147 paired Mann-Whitney). Similar results were obtained setting the expansion threshold at 16 or 32.
148 The number of PT1 expanded TCR alpha and TCR beta sequences was highly correlated
149 (Spearman's Rho = 0.85, p<0.0001, **Supplementary File 3**).

Figure 2

A

B

C

150

Figure 2: Sensitization with DPC induces a transient expansion in the frequency of a small subset of the TCR repertoire.

(A) The abundance distribution of TCRs at PS and PT1. All samples were subsampled to the same number of TCRs (28,000). Each unique TCR is represented by a dot, and the axes represent the number of times it is observed in the PS (x-axis) and PT1 (y-axis) sample of the same individual. The left and center panels represent two representative individuals. The right panels show one representative healthy volunteer at zero and two weeks (equivalent timings to PS and PT1). The plots for all individuals are shown in **supplementary file 3**. The pink dots identify a population of TCRs absent in the PS sample and expanded (abundance ≥ 8) in the PT1 sample. The blue dots identify a population of TCRs absent in the PT1 sample and expanded (≥ 8) in the PS sample. The numbers indicate the percentage of PT1 expanded TCRs (pink) and PS expanded TCRs (blue). **(B)** The abundance distribution profile of TCRs present at PT1 and absent at PS corresponding to the left panel in A (orange), middle panel (green) and right panel (gray). The y axis shows the proportion of the TCRs which are found at the abundance indicated by the x-axis. **(C)** The distribution of the percentages of PT1 expanded (≥ 8) TCRs in healthy volunteers (n=5) and in sensitized individuals (n=22), and the distribution of the percentages of PS expanded (≥ 8) TCRs in sensitized individuals (n=22), all subsampled as in (A). Bars show paired Mann-Whitney comparisons.

_____

After the initial increase post-sensitization, the number of expanded TCRs remained rather constant over the later time points. There was no evidence that the total number of expanded TCRs increased with time, despite the fact that individuals were exposed to repeated therapeutic stimulation with sensitizer on a weekly basis for the period of the study in addition to the patch test applications (**Figure 1A**) (Kruskal-Wallis rank sum test, p=0.92 alpha and p=0.36 beta). However, this apparent overall stability hid dramatic dynamic changes in the frequency of individual TCRs within individual patients. The majority of PT1 (2 week) expanded TCRs decreased or returned to baseline at subsequent time-points (**Figure 3A**). The majority of PT2 expanded TCRs present at six weeks were not expanded at two weeks, peaked at six weeks, and decreased or returned to baseline by the time the PT3 sample was taken at around 24 weeks (**Figure 3B**). These dynamics are shown for the beta chain sequences of ten patients for whom all four time points were available (the corresponding analysis for five healthy volunteers is in **Figure 3C**). The alpha chain sequences of the same patients behaved similarly (**Supplementary File 4**). The exposure to repeated doses of DPC therefore induced large, but predominantly transient, changes in the frequencies of a small proportion of the TCRs.
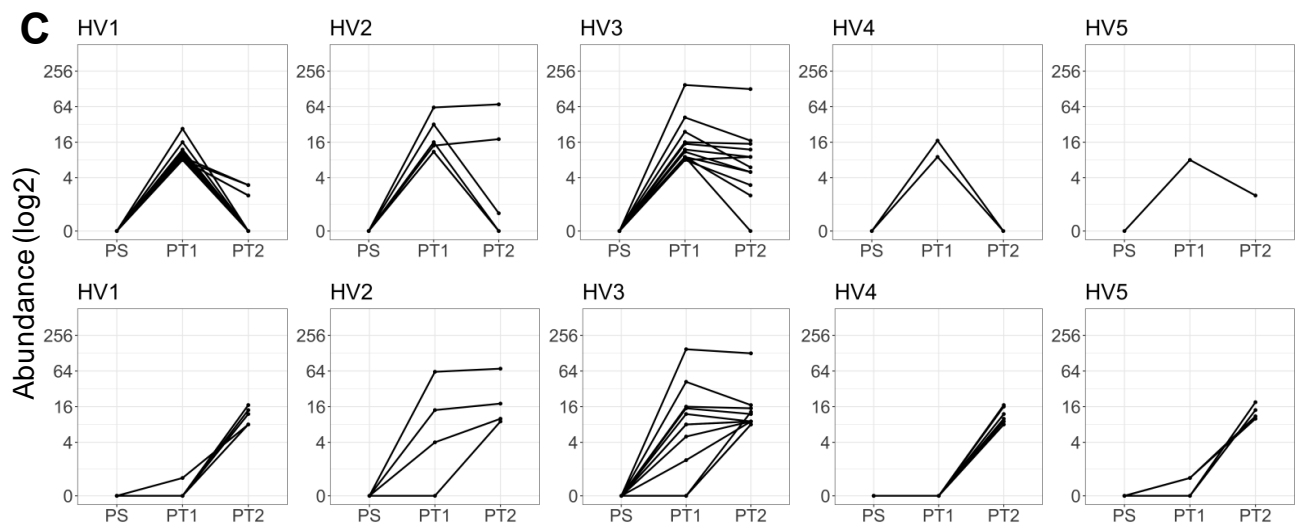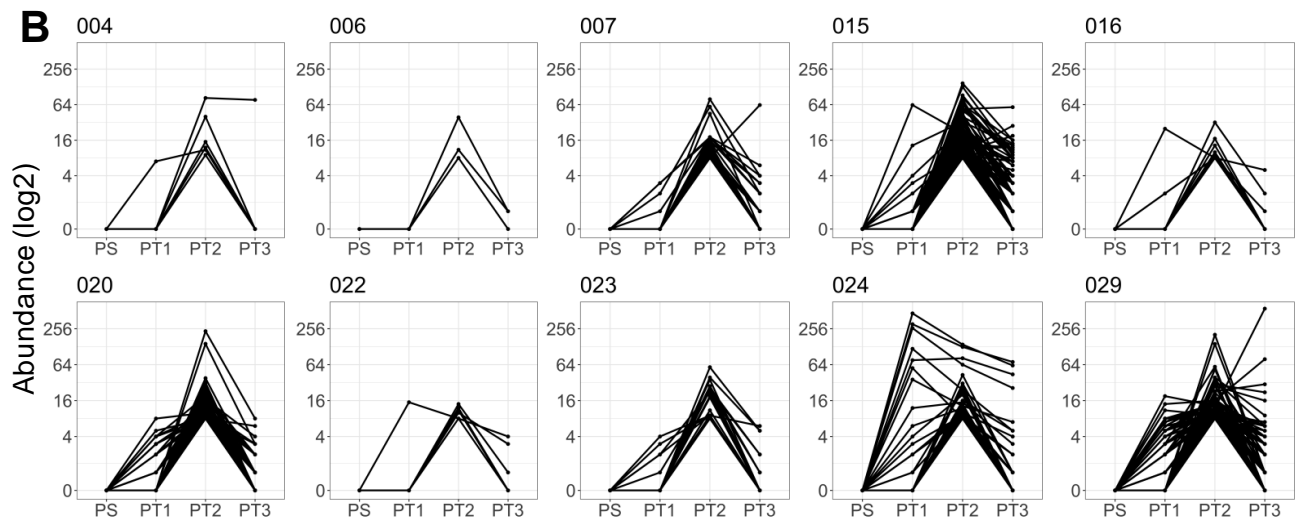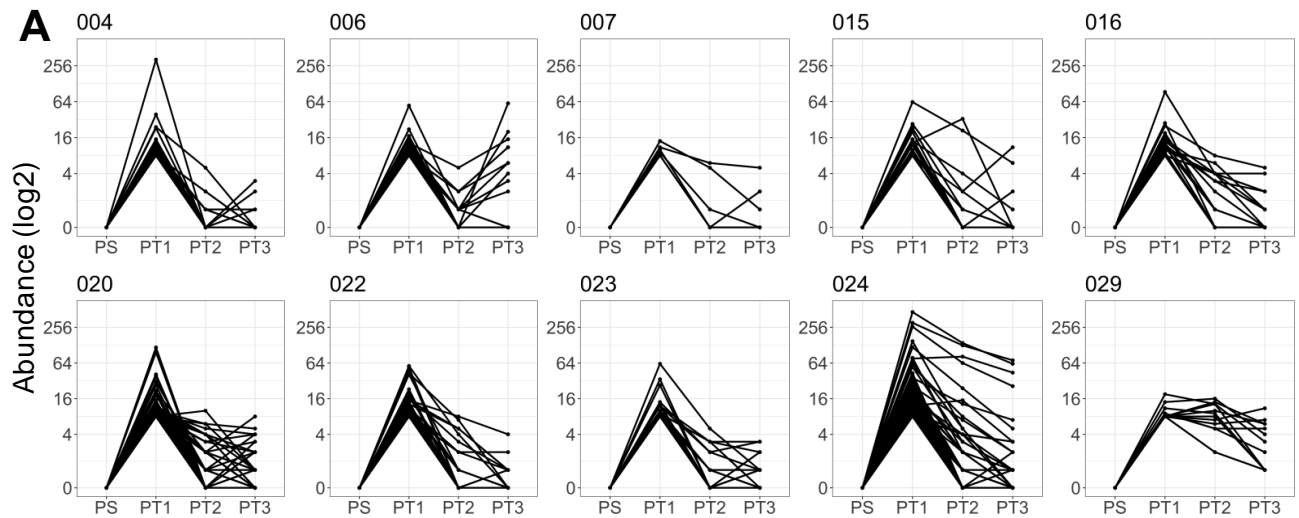
Figure 3: Dynamic changes in TCR frequency following sensitization.

(**A**) The abundances of the PT1 expanded (threshold ≥ 8) beta TCRs at the four time points: PS, PT1, PT2, PT3. Each panel is a different patient (n=10). (**B**) The abundances of the PT2 expanded (threshold ≥ 8) beta TCRs at the four time points: PS, PT1, PT2, PT3. Each panel is a different patient (n=10). (**C**) Equivalent time points (0 weeks, 2 weeks and 6 weeks) for five healthy volunteers. Top row is PT1 expanded beta TCRs; bottom row is PT2 expanded beta TCRs.

_____

TCR expansion after exposure to DPC correlates with the magnitude of skin sensitization.

We hypothesized that the expanded TCRs identified above might be functionally related to development of ACD. Exposure to DPC induced skin sensitization (patch test scores of + or higher) in almost all individuals but the magnitude of the response varied significantly between individuals (**Figure 4A**). Interestingly, the maximum response was usually observed at the first patch test, and declined or remained constant thereafter despite repeated exposure (**Figure 4B**). The sensitization reaction, therefore, like the number of expanded TCRs, did not continue to increase despite repeated exposure to antigen. In consequence, the magnitude of the response was very diverse at the beginning (+++, ++ or +) but converged towards a score of + or below by Week 24.

We plotted the number of PT1 expanded TCRs (abundance ≥ 8) in individuals with varying strengths of sensitization as a function of the initial skin response recorded at the site of application (**Figure 4C, left panels)** or at the first patch test (**Figure 4C, center panels**). The number of PT1 expanded TCRs was positively correlated to the patch test score. The correlation was positive but did not reach significance at an expansion threshold of 4, but remained significant when using a threshold abundance of 16 or 32. In contrast, there was no significant association between the number of PS expanded TCRs and the PT1 patch test score (**Figure 4C, right panels).** Although we measured the proportion of expanded TCRs, and not the absolute number, it remained possible that the total number of TCRs in each sample could affect the percentage of expanded TCRs. However, there was no significant correlation between the proportion of PT1 expanded TCRs (abundance ≥ 8) and the total number of TCRs sequenced in each sample (Spearman's correlation rho=0.18 (p=0.4) and rho=0.22 (p=0.3) for alpha and beta respectively). We also carried out repeated (10 times) subsampling of each sample to the size of the smallest sample. We observed a mean positive correlation (Spearman's rho) between the patch test scores and the percentage of PT1 expanded TCRs in the subsamples at a threshold of 8 (0.4 (alpha) and 0.3 (beta)), but the p value did not reach significance (p=0.18 and 0.22 respectively). At a threshold of 16, the correlations were 0.54 (p=0.04) and 0.32 (p=0.2), and at a threshold of 32, the correlations were 0.58 (p=0.01) and 0.61 (p=0.006) for alpha and beta respectively. Overall, the qualitative pattern of greater number of PT1 expanded TCRs remained the same after subsampling although the smaller data sets did alter the magnitude of the correlations and the threshold at which they became significant.

The correlation between the number of expanded TCRs at all time points (in each case measured as change relative to pre-sensitization frequency) and the sensitization/patch test scores at all time points is summarized in **Figure 4D.** As illustrated above, the numbers of expanded TCRs at PT1 were correlated with the strength of the reaction recorded at the sensitization site, and with the patch test score at PT1 (two weeks), as well as PT2 (six weeks). The correlation was lost at PT3 (24 weeks), perhaps reflecting the greatly decreased range of patch test scores at this time point (**Figure 4B**).

10

Figure 4

A

Pre-sensitization	No Reaction -	Weakly Sensitized +	Strongly Sensitized ++	Extremely Sensitized +++

B

PT1 score +++ (n=4)

PT1 score ++ (n=6)

PT1 score + or - (n=11)

C

$R = 0.52$, $p = 0.029$	$R = 0.64$, $p = 0.004$	$R = 0.26$, $p = 0.31$	alpha
Sensitization score	PT1 score	PT1 score	
$R = 0.44$, $p = 0.069$	$R = 0.58$, $p = 0.011$	$R = 0.27$, $p = 0.28$	beta
Sensitization score	Patch Test Score / PT1 score	PT1 score	

D

230

**Figure 4: TCR expansion after exposure to DPC correlates with the magnitude of allergic contact dermatitis.**

(A) Photographs showing examples of the varying levels of skin reaction observed in response to DPC; the reactions were classified according to standards set by the International Contact Dermatitis Research Group (no reaction (-), +, ++, +++). **(B)** The changes in patch test scores during treatment in patients with PT1 score of +++ (n=4, **left panel**), ++ (n=6, **middle panel**), and + or - (n=11, **right panel**). **(C) Left panels** The number of PT1 expanded (≥ 8) clones are plotted against the sensitization score. **Center panels** The number of PT1 expanded (≥ 8) clones are plotted against the PT1 patch test score. **Right panels** The number of PS expanded (≥ 8) clones are plotted against the patch test score at PT1. The blue line indicates the best fit linear model, with the model's 95% confidence intervals in grey. The inset text shows the Spearman's correlation coefficient, rho. **(D)** Correlation matrix representing the Spearman correlation between the number of PT expanded TCRs and the reaction recorded at the sensitization site or the patch test scores at each timepoint. The color and size of each square correspond to Spearman's rho, and non-adjusted p-values are shown.

_____

The expanded TCRs show characteristics of antigen-driven responses.

We hypothesized that the population of TCRs that are found at increased frequency post-exposure to DPC may be enriched for T cells which bind to DPC, or DPC-modified peptides. Antigen-specific sets of TCRs frequently share sequence features, including skewed use of V and J regions, and similarities in CDR3 sequence (Dash et al., 2017; Davis et al., 1995; Glanville et al., 2017; Pogorelyy et al., 2019; Sun et al., 2017; Thomas et al., 2014). The relative V and J gene usage profiles within the expanded set of TCRs compared to the pre-sensitization repertoire for that individual are shown for each patient in **Figure 5**. We used a non-parametric bootstrapping approach to determine which V and J genes were statistically significantly skewed in the repertoire of the expanded TCRs. We compared the observed proportion of each V and J gene in the PT1 expanded TCRs (≥ 8) with 1000 random sets of the same number of TCRs sampled from the pre-sensitization repertoires of the same individuals. V and J genes that ranked in the top 50 out of 1001 were considered significantly under-represented at the 0.05 significance level, and genes in the bottom 50 ranks as significantly over-represented. Several examples of skewed V and J gene usage were observed, both in TCR alpha and TCR beta (pink dots). Due to the relatively small number of expanded TCRs in some patients, under-represented genes were very common as a result of sampling, and hence less statistically robust. We therefore show only over-represented V and J genes. In addition, genes that were over-represented by a similar analysis on the set of all expanded TCRs (generated by combining the individual patient expanded sets and taking unique TCRs) are also shown (**Figure 5**, pink gene names). Interestingly, some V and J regions were skewed in several different individuals, suggesting some common driver of V/J gene usage, despite the fact that the individuals were not related.
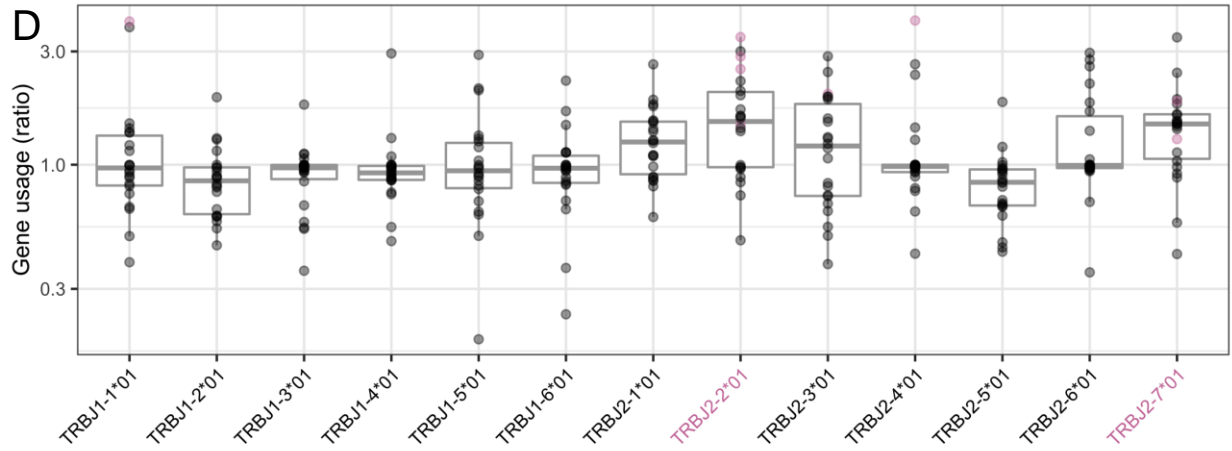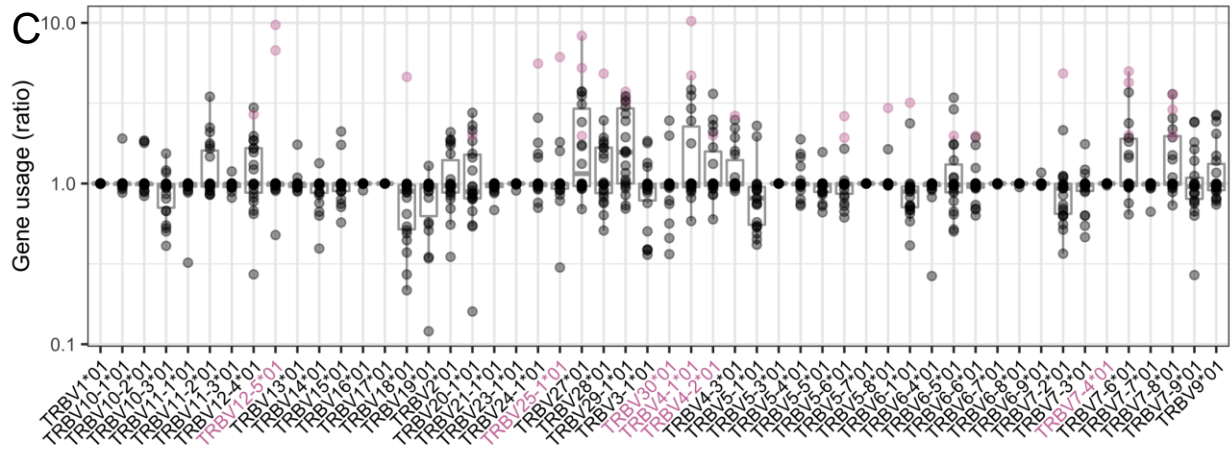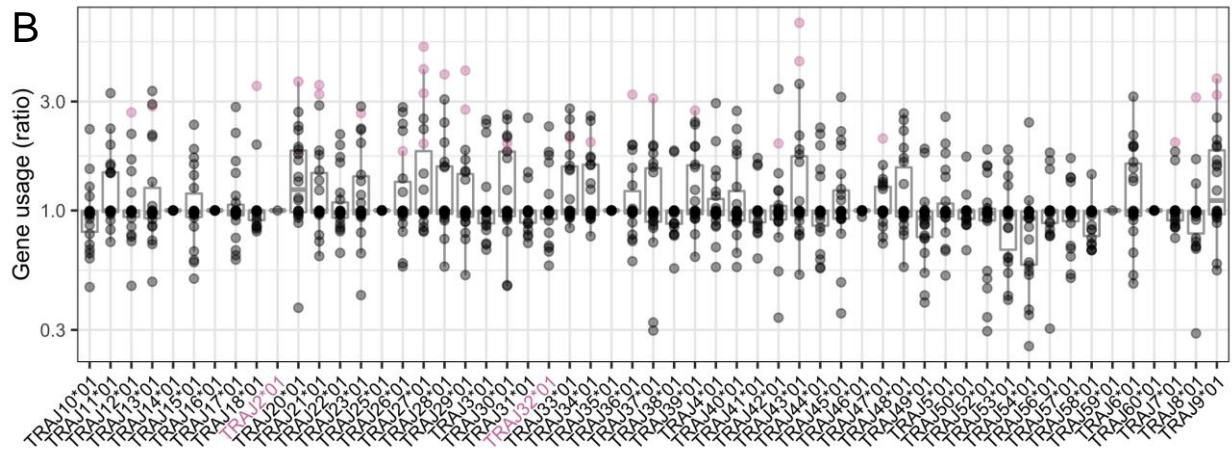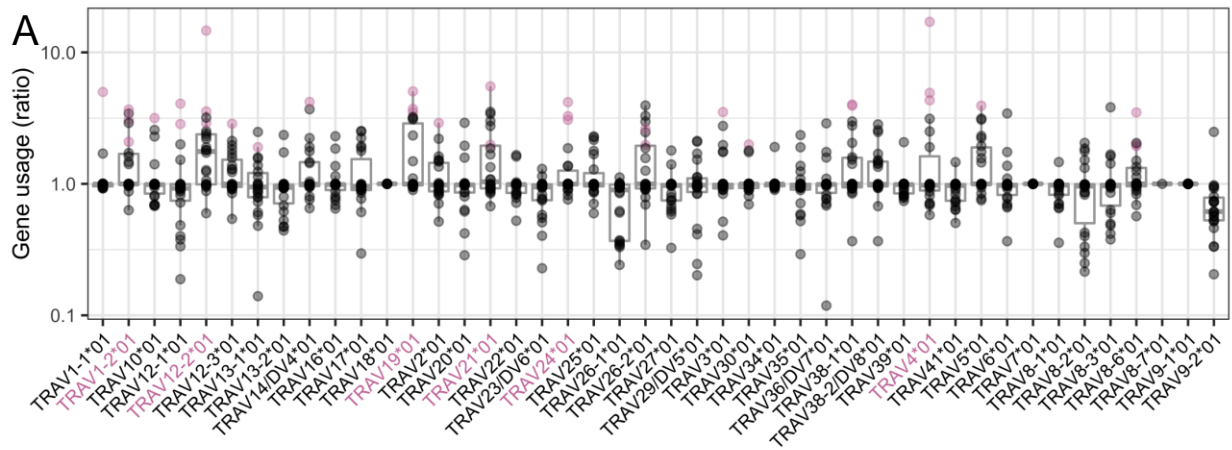
Figure 5: The expanded TCRs show characteristics of antigen-driven responses in their V and J gene usage.

Relative frequency of V and J alpha and beta gene usage in the set of PT1 expanded TCRs (≥ 8) from 22 individuals, compared to the frequency in their respective pre-sensitization repertoires. Each dot is a patient. Genes significantly over-represented in the expanded set (see text for statistical test) are colored pink. Under-represented genes are not included in this figure, since the small number of expanded TCRs in some patients resulted in a large but less meaningful set of under-represented genes due to sampling. Genes colored pink on the x-axis are those that were significantly over-represented in the combined expanded set (1858 unique alpha TCRs and 2019 unique beta TCRs).
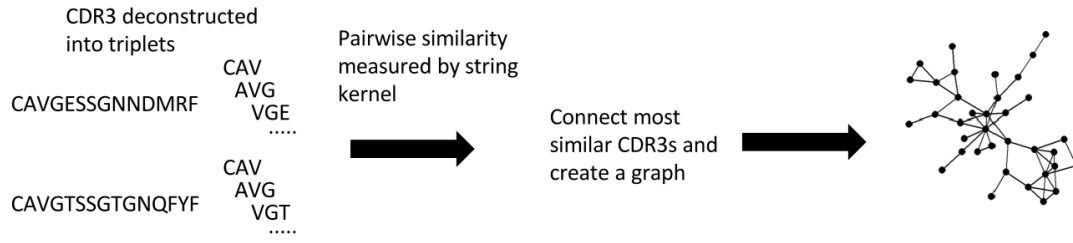
_____

We also looked for potential clustering of CDR3 sequences of the expanded TCRs (**Figure 6**). We have previously shown that amino acid triplets (sequences of three adjacent amino acids within the CDR3 region) can predict antigen specificity (Sun et al., 2017). We therefore compared the pairwise similarity of all expanded CDR3s using a metric that quantifies the number of shared triplets between two sequences, normalized for sequence length (an example of a string kernel in the machine learning literature (Shawe-Taylor and Cristianini, 2004). We converted the matrix of pairwise similarities into a network (**Figure 6A**), by connecting all those TCRs with a similarity above a given threshold (75%). As control, we performed the same analysis on same-sized sets randomly sampled either from the combined pre-sensitization repertoire (**Figure 6B,C (ii)**) or from the combined repertoire of the healthy volunteers (**Figure 6B,C (iii)**). The expanded TCRs formed significantly more large clusters of "related" TCRs than either control sets (**Figure 6B,C (i)**). We selected the largest cluster of CDR3 beta sequences (**Figure 6D**) and carried out an alignment (summarized in **Figure 6E**, full alignment **Supplementary File 5**). The sequences showed a high level of similarity consistent with belonging to a set of TCRs with shared specificities (Dash et al., 2017; Glanville et al., 2017).

Taken together, the skewing of V and J genes, and the presence of clusters of similar TCRs were strongly suggestive that the expanded TCRs were enriched for TCRs responding to a limited number of specific epitopes.

14

Figure 6

A

CDR3 deconstructed
into triplets

CAVGESSGNNDMRF

CAV
AVG
VGE
.....

Pairwise similarity
measured by string
kernel

Connect most
similar CDR3s and
create a graph

CAVGTSSGTGNQFYF

CAV
AVG
VGT
.....

B

(i)

(ii)

(iii)
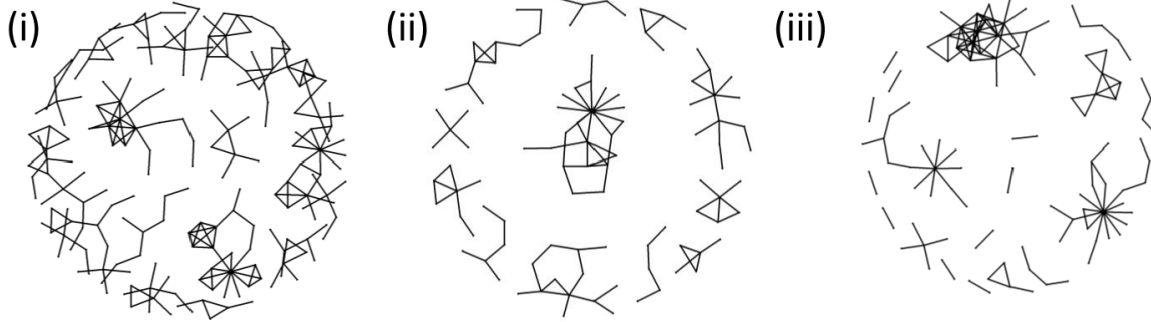
Percentage of TCRs in cluster	15	9.5+/-0.4	11.6+/-0.5
Number of clusters	28	20+/-0.9	23+/-0.95

C

(i)

(ii)

(iii)
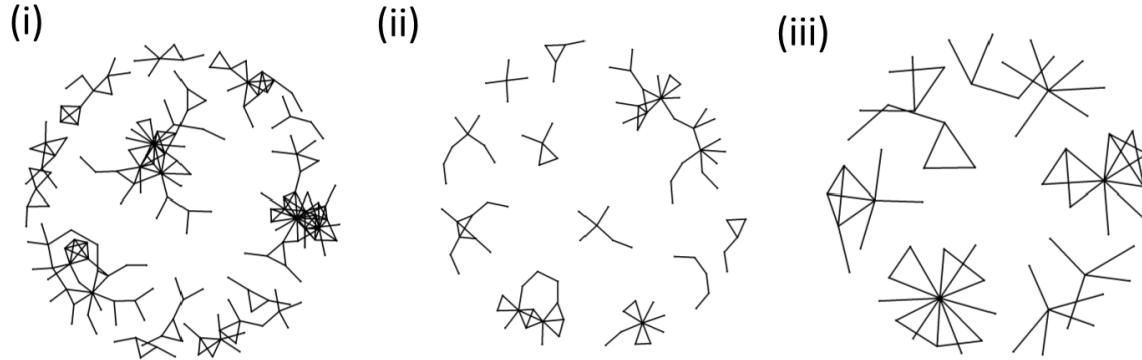
Percentage of TCRs in cluster	9.2	6.4+/-0.3	6.0+/-0.3
Number of clusters	14	12.6+/-0.4	11.6+/-0.5

D

E
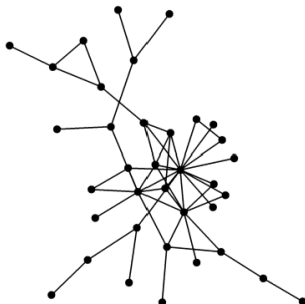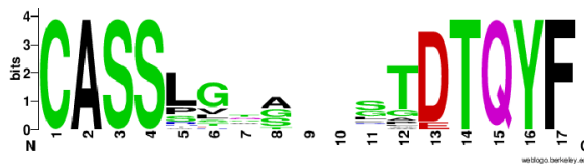
Figure 6: The expanded TCRs show clustering characteristics of antigen-driven responses.

(A) Diagram illustrating the similarity graph construction process. Individual CDR3s are deconstructed into overlapping series of contiguous amino acid triplets, and the pairwise similarity between two CDR3s is calculated as the normalized string kernel. Two CDR3s which have a pairwise similarity of >0.75 are connected by an edge. **(B)** Clusters formed from the CDR3 sequences of **(i)** the PT1 expanded alpha TCRs (≥ 8), **(ii)** an equal-sized (1858) set of alpha TCRs sampled randomly from the combined pre-sensitization repertoires of the same patients, and **(iii)** a size-matched set randomly sampled from the combined healthy volunteer alpha TCRs. The numbers under each network diagram show the percentage of the 1858 TCRs which are incorporated in a cluster, and the number of clusters. The numbers for the pre-sensitization and heathy volunteers show the average +/- standard error of the mean for each parameter. **(C)** As (B), but for beta sequences (2019 expanded TCRs, or same number of control TCRs). **(D)** The largest (35 unique CDR3s) cluster of PT1 expanded TCR beta sequences, from panel (B)(i). **(E)** An alignment of CDR3 sequences from the cluster shown in panel (D). The alignment is illustrated as a sequence logo (https://weblogo.berkeley.edu/logo.cgi). The full alignment is shown in **Supplementary File 5**.

_____

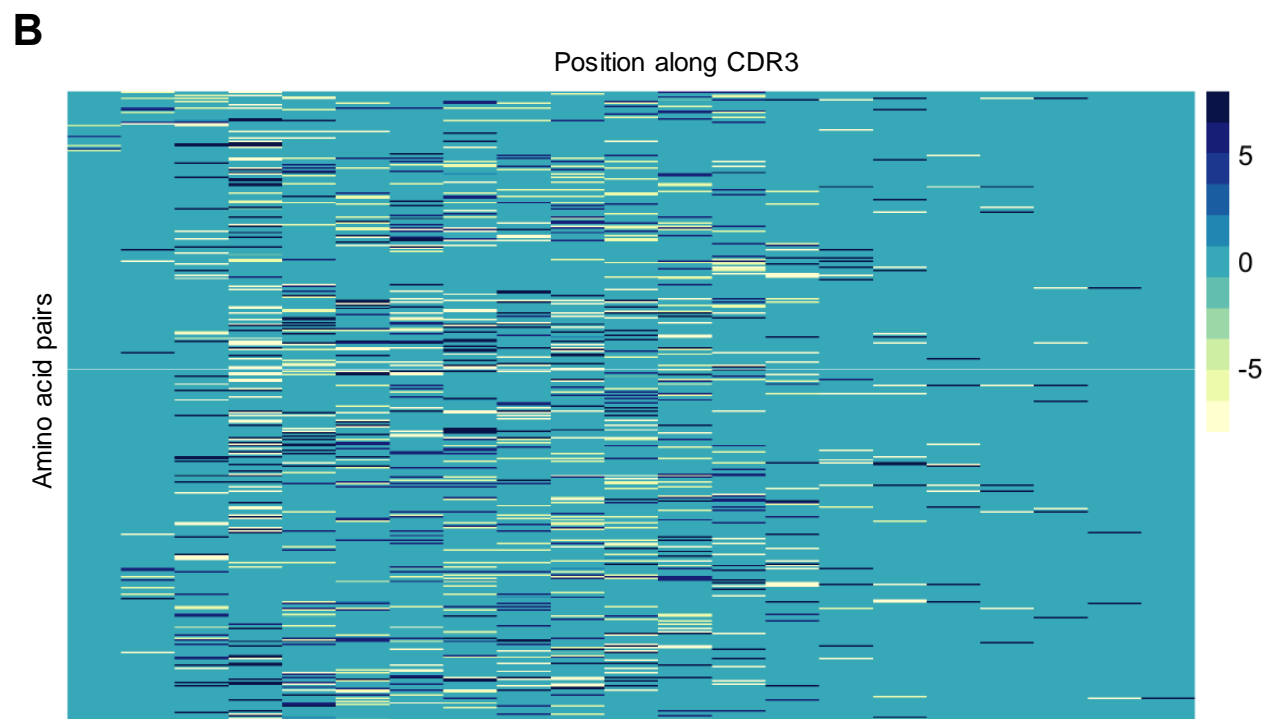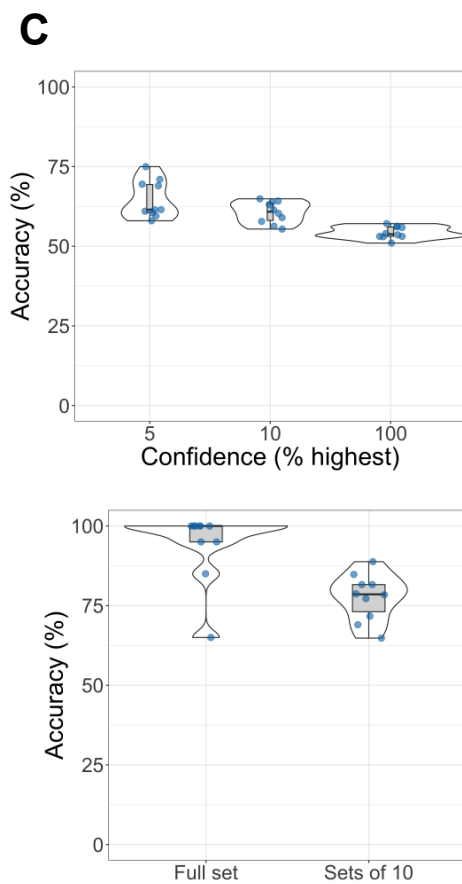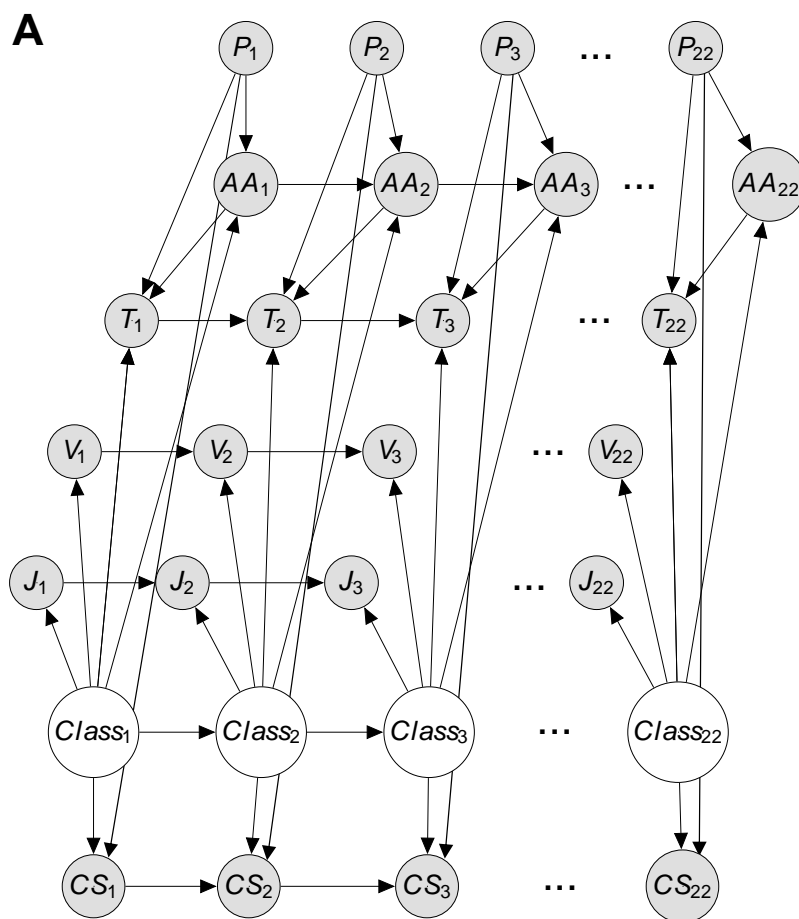**A Dynamic Bayesian Network can predict sensitization based on TCR sequence.**

The skewed V/J usage and the TCR clustering are indicative of an antigen specific response. We therefore explored whether the repertoire of expanded TCRs was sufficiently distinct from that of the unselected repertoire so that it could be used to distinguish DPC-expanded TCRs or sets of TCRs from the unexpanded repertoire. We used a Dynamic Bayesian network (DBN) (Dagum et al., 1992; Murphy and Mian, 1999; Murphy and Russell, 2002; Pearl, 1988; Yao et al., 2008) a model we have developed to interrogate antigen specificity in TCR sequences. The DBN is a probabilistic graphical model, which provides a flexible classification tool that can incorporate heterogeneous data (e.g. sequences as well as V/J usage).

We constructed a DBN to classify TCR beta CDR3 sequences into one of two classes: DPC-related CDR3s, and randomly sampled pre-sensitization CDR3s from the same individuals. To construct the training/test sets for the model, we used the PT1 expanded CDR3 sequences (≥ 8) for the DPC class, which were at most 22 amino acids long (2019 beta sequences from 22 patients), and for the control class, a randomly generated set of the same number of TCRs from the combined pre-sensitization sequences. CDR3 sequences in the expanded set were excluded from the pre-sensitization (control) training set. The length of CDR3 sequences used in the model was capped at 22 in order to manage the computational complexity of the algorithm, while still utilizing all expanded sequences. To account for the variable length of the CDR3 sequences, the sequences were aligned by the first Cysteine of the CDR3 on the left, up to the final Phenylalanine of the CDR3, then 'completed' to length 22 using a dummy variable ('amino acid number 21'). The DBN took as input the amino acid in each position in the CDR3 (converted to an integer 0-21 for each amino acid or dummy), the V and J genes, as well as position specific triplet scores and class scores (as explained in Materials and Methods). The proposed probabilistic dependencies between these sequence features and antigen specificity are encoded into the network structure by directed edges (**Figure 7A**). Further details of the DBN and how it was trained and tested are provided in Materials and Methods.

One of the key features of the DBN is that each 'slice' of the network is position specific. This enables modelling local as well as global sequence features. For example, **Figure 7B** demonstrates the relationship between neighboring amino acids in specific positions in the CDR3 sequence and antigen specificity. The probability of observing a specific amino acid in a particular position given its neighbors differs between DPC-expanded sequences and control sequences. Both over and under-represented pairs of amino acids can be seen, in particular in the middle of the CDR3. Such relationships are utilized by the model in classification.

16

345   The DBN classifier could classify the full DPC/control test sets with mean accuracy of 94% from 10
346   repeats of 10-fold cross validation, and sets of ten sequences with mean accuracy 77.7% (**Figure**
347   **7C** upper panel). Model confidence in classifying individual sequences correctly, taken as the
348   difference in the log likelihood between the DPC and the control models for each sequence, varied
349   between different test sets and sequences. Where the DBN was asked to classify every sequence
350   regardless of confidence level, the mean accuracy was 54.3%. When taking the 5% or 10% most
351   confident assignments, individual sequences were classified with mean accuracy of 64.7% and
352   60.6% respectively, from 10-fold cross validation (**Figure 7C** lower panel). The DBN provides
353   mechanistic insight into which features are critical for classification, in addition to confidence bounds
354   on its decisions, since the probabilities used by the model in classification are transparent.

A

C

B

Position along CDR3

Amino acid pairs

355

Figure 7: A Dynamic Bayesian Network can predict sensitization based on TCR sequence.

356

357 **(A)** The directed acyclic graph depicts the dynamic Bayesian Network (DBN) structure, unrolled over 22 time
358 slices (positions). Directed edges capture probabilistic dependencies. P_i indicates position i along the CDR3
359 sequence; AA_i the amino acid in position i; T_i is the triplet score for the triplet of amino acids in positions
360 $< i - 2, i - 1, i >$; V_i and J_i are the V and J genes (constant for each sequence), CS_i the class score at position
361 i, and $Class_i$ determines whether the sequence comes from the DPC-related expanded set, or the control set.
362 **(B)** The probability of observing pairs of neighboring amino acids differs between DPC-related sequences and
363 control sequences from the pre-sensitization repertoire of the same individuals. Each column in the heatmap
364 corresponds to a position along the CDR3 sequence, each row to an ordered pair of amino acids (total 400). If
365 row i in the heatmap corresponds to amino acid pair $< X, Y >$, then position $< i, j >$ in the matrix is the ratio of
366 the probability of observing amino acid Y in position $j+1$ in the expanded sequences against the probability of
367 observing Y in the same position in an equal-sized random sample of control sequences, given amino acid X
368 has been observed in position j. **(C)** The upper panel shows the mean classification accuracy for classifying
369 the full DPC/control test sets, and sets of ten DPC/control sequences. Each dot depicts the mean of one the
370 train-test sets from 10-fold cross validation over ten generations of the model. The lower panel shows mean
371 classification accuracy for individual sequences. 5% confidence refers to the top 5% of sequences with
372 greatest log likelihood difference between the models, and similarly for 10%. 100% is the accuracy when
373 classifying every sequence. Each training set consisted of 3618 expanded sequences and control sequences
374 in equal proportions, and the test sets 402 sequences in equal proportions (201 expanded and 201 control).

375 _____

Discussion

377 The results presented above report the first comprehensive analysis of the TCRrep in the context of
378 controlled exposure to a contact sensitizer in humans. The key findings are that the response to
379 sensitizer is accompanied by a dynamic, robust polyclonal increase in abundance of a defined set of
380 T cell receptor genes which presumably reflects clonal expansion of antigen specific T cells in
381 response to DPC. Notably, the breadth of the response, as captured by the number of TCRs that
382 increase in frequency, is very diverse between individuals, and predicts the degree of sensitization.
383 Furthermore, the response of individual TCRs, which reflect individual T cell clonal dynamics, is
384 transient, with most TCRs returning to low frequencies, or disappearing by the subsequent
385 timepoint.

386 The immunological mechanisms that drive ACD have been studied in detail (see for example
387 (Kimber et al., 2012)). The dose and frequency of exposure are both key parameters in determining
388 the strength of the response (Friedmann, 2006, 2007), although it is clear that the full impact of
389 different factors on the observed variance in the population is still not fully understood, and is one
390 limitation in accurate prediction of allergy to chemical exposure in the context of consumer safety
391 (Basketter and Safford, 2016). There is widespread agreement that activation of both CD4+ and
392 CD8+ antigen specific T cells play key roles, although antibody may also be important (Singleton et
393 al., 2016).

394 The nature of the molecular interaction between the sensitizer, which is usually a chemical hapten
395 that reacts with macromolecules including proteins in the skin following exposure, remains much
396 less well-understood than for microbial or viral peptide antigens. There are no MHC tetramer or
397 multimers which can be used to identify DPC or indeed any hapten-specific T cells. Nevertheless, a
398 number of lines of evidence support our hypothesis that the TCRs that increase in frequency
399 following sensitization represent an antigen-specific response. The observed changes from zero to 8
400 are unlikely to be due to sampling effects; in fact, modelling sampling as a Poisson process
401 indicates that changes from zero to 8 or more have individual probabilities of <0.05. The observed
402 changes are also unlikely to arise from exposure to unknown antigens (for example infectious
403 agents) since the number of expanded TCRs at the first time point post-sensitization is greater than
404 the number of expanded TCRs observed in unsensitized individuals sampled at similar time points,

405   for the great majority of the patients tested. The functional link between TCR expansion and DPC
406   exposure is also strengthened by the observed statistical correlation between the number of
407   expanded TCRs and the vigor of sensitization, as measured by the patch test. Moreover, the
408   expanded set of TCRs show strong evidence of V and J gene skewing, and of increased CDR3
409   clustering, both well-established signatures of an antigen-specific T cell response (Thomas et al.,
410   2014; Sun et al., 2017a; Davis et al., 1995; Glanville et al., 2017; Dash et al., 2017). Finally, these
411   features are shown to be discriminatory enough to allow classification of TCRs into DPC-related and
412   healthy volunteer TCRs by the Dynamic Bayesian Network. Taken together, this set of observations
413   suggest that DPC, perhaps in the form of a set of modified-self peptide adjuncts, stimulates a
414   transient expansion of T cells carrying a defined set of related TCRs. The observation that TCR
415   clustering, V region enrichment and DBN classification could be observed across a panel of
416   unrelated individuals is particularly intriguing, and suggests that hapten-specific responses may be
417   less dependent on MHC matching than conventional peptide-specific responses. However, further
418   more detailed study is required to determine the molecular target of the DPC-responsive TCRs.

419   DPC is considered a potent sensitizer (Stute et al., 1981; Mose et al., 2017b). Nevertheless, we
420   noted a wide range of quantitative responses in different individuals, at least as measured by
421   standard patch test results. This was reflected in a wide range of expanded TCRs, and the number
422   of expanded TCRs at the first post-sensitization sample (two weeks) showed strong correlation to
423   the strength of the response. The reasons for this inter-individual variation are unknown, but could
424   reflect inter-individual differences in immune response (Brodin et al., 2015), or potentially differences
425   in factors that control hapten penetration, such as skin thickness or composition (Reynolds et al.,
426   2019). Understanding the factors that determine this variation may be important in developing novel
427   approaches to ACD risk prediction (MacKay et al., 2013; Maxwell and Mackay, 2008).

428   In our study, low responders were not boosted by repeated exposure to DPC over many months. In
429   fact, the response was usually maximal at the first patch test, suggesting that regulatory
430   mechanisms come into play to limit the response in vivo. Similarly the initial TCR expansion did not
431   continue to increase despite repeated exposure to antigen, and indeed the majority of TCRs showed
432   very transitory responses, with individual TCR frequencies falling to around pre-sensitization
433   frequencies by the next time point. Similar rapid expansion and subsequent contraction has been
434   observed in response to live attenuated yellow fever vaccine (DeWitt et al., 2015; Pogorelyy et al.,
435   2019), one of few examples where TCR repertoire has been studied before and after challenge in a
436   human setting. The latter study (Pogorelyy et al., 2018) precisely documents changes in TCR
437   frequency in three pairs of twins, at several time points before and after exposure to a single dose of
438   the live attenuated YFV 17D vaccine. The study documented the expansion and then contraction of
439   several hundred TCR genes, which reflected the clonal expansion, and subsequent contraction of a
440   polyclonal set of vaccine-specific T cells. However, in this case antigen was delivered as a single
441   dose of vaccine, which gives rise to systemic but very transitory viremia. T cell contraction in the
442   vaccine context may therefore reflect the rapid disappearance of antigen. In contrast, the patients in
443   the current study were exposed to repeated doses of DPC weekly over the course of many months
444   for their therapeutic benefit. The mechanisms which limit the DPC response are therefore more
445   likely to be due to intrinsic regulatory pathways (for example Treg induction), or changes in intrinsic
446   migratory pathways rather than simply reflect antigen disappearance. We noted that a second wave
447   of TCRs appeared at increased frequency at PT2, six weeks post sensitization. This set of "late"
448   TCRs were almost all distinct from the "early" peak at week 2. Furthermore, there was no correlation
449   between the magnitude of the patch test score at PT1 and the number of TCRs expanded at PT2.
450   Additional experiments will be needed to explore whether this set of late TCRs represents part of a
451   regulatory mechanism, which regulate and limit further T cell expansion during chronic exposure to
452   DPC.

453   In conclusion, this study is the first analysis of in vivo TCR repertoire changes in response to a
454   chemical allergen, and is one of only a handful of studies that document in vivo longitudinal changes

455 in TCRrep in response to immunization in humans. We cannot rule out that the immune response in
456 this population is different from healthy individuals, since all patients suffered from some form of
457 alopecia, which is believed to have an autoimmune aetiology (Trüeb and Dias, 2018). Nevertheless,
458 DPC is unlikely to bear any relation to the autoimmune target in alopecia, since similar therapeutic
459 responses (hair growth) can be observed in patients with alopecia treated with other completely
460 unrelated contact sensitizers. While the qualitative balance of immune response may be influenced
461 by the underlying autoimmune background, the specificity of the TCR repertoire is likely to reflect
462 fundamental features of the response to chemical haptens. The study confirms our previous in vitro
463 findings, that the response even to a simple chemical such as DPC is polyclonal involving dozens or
464 even hundreds of TCRs. The study also highlights the dynamic nature of the TCR repertoire. Further
465 studies will be required to unravel the complex mechanisms that regulate the immune response to
466 chronic antigen exposure.

467 **Materials and methods**

468 **Resource table**

Resource	Designation	Source or reference	Identifier	Additional information
Software, algorithm	Decombinator V4	https://github.com/innate2adaptive/Decombinator	RRID: SCR_006732	This software suite is under active development; latest versions available at the github site.
Other	TCRseq protocol	Uddin I, Woolston A, Peacock T, Joshi K, Ismail M, Ronel T, Husovsky C, Chain B. Quantitative analysis of the T cell receptor repertoire. Methods Enzymol. 2019;629:465-492. doi: 10.1016/bs.mie.2019.05.054. Epub 2019 Jun 20. PMID: 31727254.		This protocol is in a continuous state of development. The full details of the current stable version including primer sequences, PCR conditions etc. are all in the attached reference. For latest development contact the corresponding author on b.chain@ucl.ac.uk

469

470 Patient recruitment

471 A total of 34 patients were recruited to this study (NRES Ethics Committee East of England -
472 Cambridgeshire and Hertfordshire [14/EE/1067]). Participants were recruited from patients who had
473 been diagnosed with alopecia, were aged between 18 and 70, identified as suitable for DPC

474   treatment by a consultant dermatologist, and were now attending their first visit to the Alopecia Clinic
475   at Salford Royal Hospital for DPC therapy. This study ran alongside patients' prescribed DPC
476   treatment (weekly doses of DPC to the scalp to induce inflammation and hair regrowth). The study
477   timeline in terms of treatment and sample collection is provided in **Figure 1A**. All participants gave
478   their informed consent to participate, and were free to withdraw from the study at any time and for
479   any reason without affecting their treatment. Patients were excluded from the study if they were
480   pregnant.

481   29 of the individuals who participated in the study provided blood samples for TCR sequencing
482   (TCRseq), for between one and four of the study time points (pre-sensitization, and at two, six and
483   24 weeks of DPC treatment). Flow cytometry data was obtained for peripheral blood mononuclear
484   cells (PBMC) from ten treated patients, and patch test data for 23 patients. The clinical response to
485   treatment (in terms of hair regrowth) and the associated immunological changes will be discussed in
486   a separate publication. A summary of the patient demographics and the samples collected is shown
487   in **Table 1**.

488   As controls for the TCR sequencing, five healthy volunteers were bled three times, at day zero, two
489   weeks and six weeks. All subjects gave written informed consent in accordance with the Declaration
490   of Helsinki. The protocol was approved by the University College London Hospital Ethics Committee
491   06/Q0502/92.

492   Sensitization and patch testing

493   Sensitization to DPC was induced by application of 2% DPC (in acetone) to a 2cm by 2cm patch of
494   skin on the upper inner arm. Sensitization at the site of application was assessed 14 days later and
495   scored as described below (sensitization score). Patch testing at a remote site (upper back) was
496   conducted two weeks (PT1), six weeks (PT2) and 24 weeks (PT3) after application of the sensitizing
497   dose of DPC. Patch testing was performed on the skin of the upper back using Finn chambers (8mm
498   inner diameter) containing 0.01% DPC in acetone. After six days, patients' reactions were scored as
499   no reaction (-), weakly sensitized (+), strongly sensitized (++), or extremely sensitized (+++)
500   according to standards set by the International Contact Dermatitis Research Group.

501   TCR sequencing

502   The α and β chains of the TCR repertoire of 29 participants were sequenced using a method that
503   starts with total RNA isolated from unfractionated whole blood, collected in Tempus™ Blood RNA
504   tubes (Thermofisher #4342792) using the manufacturer's protocol for RNA extraction. The pipeline
505   introduces unique molecular identifiers attached to individual cDNA molecules to provide a
506   quantitative and reproducible method of library preparation. Full details for both the experimental
507   TCRseq library preparation and the subsequent computational analysis (V, J and CDR3 annotation)
508   using Decombinator are published in (Oakes et al., 2017b; Uddin et al., 2019).

509   Flow cytometry

510   Peripheral blood mononuclear cells were isolated from 30mL whole blood (diluted 1:1 in PBS) from
511   ten patients layered over an equal volume of Histopaque 1077 (Sigma Aldrich) according to the
512   manufacturer's instructions. Cells were stored at a concentration of $5x10^7$ cells/mL in 10%
513   DMSO/90% human AB serum (Sigma Aldrich) at $-80^{o}C$ until required.

514   Flow cytometric analyses were performed on previously frozen cells using antibodies obtained from
515   eBioscience, with single-stained controls used for compensation. Naïve and memory CD4+ and
516   CD8+ T-cell subsets were identified as previously described (Appay et al., 2008). Naïve cells were
517   defined as CD45RA+ and CD27+; central memory as CD45RA- CD27+; effector memory as
518   CD45RA- CD27- and EMRA as CD45RA+ CD27- . Flow cytometry was performed on a minimum of

519   10,000 cells using a FACS-calibur (Becton Dickinson, Mountain View, CA) and data analysis
520   performed in FlowJo (TreeStar) using standardized gating across all samples.

521   Statistical and mathematical analysis

522   Statistical analyses were performed using the statistical programming language R [R version 4.0.2
523   (2020-06-22)]. Mann-Whitney U tests were used to compare between two unmatched groups and
524   paired t-tests between two paired groups. All statistical comparisons between more than two groups
525   were done using Kruskal-Wallis non-parametric tests with post hoc Dunn Test and Benjamini-
526   Hochberg correction for multiple testing. Statistical significance in all tests was accepted above the
527   0.05 threshold.

528   To calculate which V and J genes were significantly over or under expressed in the DPC-expanded
529   TCR sets, at both the individual patient level and for the entire expanded set, we generated 2*1000
530   independent random samples of equal-sized sets from the pre-sensitized individual/combined
531   population, calculated the ratio between the two, and compared this with the ratio derived from the
532   set of interest against a further 1000 random simulations. A significance level of 0.05 was then
533   achieved for genes that ranked in either the top 50 'ratios' (under-represented) or bottom 50 in the
534   list (over-represented).

535   TCR clustering

536   The CDR3 protein sequences of expanded TCRs were identified using the package CDR3translator
537   (https://github.com/innate2adaptive/Decombinator). The pairwise similarity between TCRs was
538   measured on the basis of amino acid triplet sharing, which was calculated using the normalized
539   string kernel function stringdot (with parameters stringdot(type="spectrum", length=3,
540   normalized=TRUE) from the Kernlab package (Karatzoglou et al., 2004). The kernel was calculated
541   as the number of amino acid triplets (sets of three consecutive amino acids) shared between two
542   CDR3s, normalized by the number of triplets in each CDR3 being compared. The TCR similarity
543   matrix was converted into a network diagram using the iGraph package in R (Csardi and Nepusz,
544   2006). Two TCRs were considered connected if the similarity index was above 0.75. A range of
545   thresholds were explored, and the lowest threshold that consistently gave few large (>3 nodes)
546   clusters using random samples of TCRs from the study was chosen. The sequences from individual
547   clusters were aligned using Aliview (Larsson, 2014), and the consensus visualized using webLogo
548   (https://weblogo.berkeley.edu/logo.cgi).

549   TCR repertoire classification using a Dynamic Bayesian network (DBN)

550   Dynamic Bayesian Networks are a type of probabilistic graphical model consisting of a directed
551   acyclic graph and a set of conditional probability distributions. The probability of the set of variables
552   (nodes) of the system X_t at time t given its state at time $t-1$ can be calculated by

$$P(X_t|X_{t-1}) = \prod_{i=1}^{N} P\left(X_t^{(i)} \,\middle|\, Pa\left(X_t^{(i)}\right)\right)$$

553   where N is the number of variables, $X_t^{(i)}$ is the i'th node in time slice t and $Pa(X_t^{(i)})$ are the parents of
554    $X_t^{(i)}$. The TCR DBN was built in MATLAB (2019b), using the Bayes Net Toolbox (Murphy, 2001). The
555   DBN took as input the position along the CDR3 sequence, the amino acid in each position, the V
556   and J genes, a position specific triplet score and a class score relative to sequence position. An
557   edge between neighboring amino acids was included in the network to model the observed non-
558   independence between neighboring amino acids in their specific sequence positions and the
559   sequence specificity. The triplet score was calculated by taking for each position the triplet
560   containing the two previous amino acids in the CDR3, and ranking it against other triplets in this
561   position in the control and DPC training sets. The triplet was given a score of 1 if it appeared more

562 frequently (in a given position) in the DPC training set than in the control training set, which
563 consisted of the same number of sequences randomly sampled from the pre-sensitization
564 repertoires of the same patients. Triplets that were more frequent in the control set were scored 2,
565 and triplets that appeared equally in the DPC and control sets were scored 1 or 2 uniformly at
566 random. Positions 1 and 2 were taken as a singleton and an ordered pair of amino acids
567 respectively and scored similarly. Triplets were chosen since they were sufficiently high-dimensional
568 to capture amino acid dependencies but remained computationally feasible. To calculate the class
569 scores, the following procedure was followed: **1** Each V gene in the training set was scored 1 if it
570 was more prevalent in the DPC set, 2 if in the control set, and 1 or 2 uniformly at random otherwise.
571 **2** The J genes were scored similarly. **3** For each sequence position, every amino acid (and an
572 additional dummy amino acid added to the end of CDR3s shorter than 22 to equalize sequence
573 lengths) was scored 1 or 2 as above. **4** Finally, the class score for position *i* was assigned 1 if the
574 total number of '1' scores obtained by Steps **1-3** and the triplets scores from positions *1,2,…,i-1* was
575 greater than the number of '2' scores; a score of 2 if the number of '2's was greater, and 1 or 2
576 randomly otherwise. Training sequences were assigned 1 or 2 in position 22 according to their
577 original class. This process ensured knowledge about the likelihood of belonging to either set could
578 be learned by the model across timeslices (positions). Class scores for the test sets were calculated
579 based on gene, amino acid and triplet frequencies in the training sets. Nodes depicting specificity
580 (DPC or control) were included as hidden (latent) variables. Inference on the network was done
581 using the Junction Tree algorithm, and parameters were initiated with Dirichlet priors and fitted to the
582 network by Expectation Maximization with a maximum of ten iterations. Two DBNs were
583 constructed, one for the DPC training set and one for the control set. To classify TCR sequences,
584 the log likelihood of each model was calculated. For sets of sequences, we calculated the sum log
585 likelihood for each model. The results of the DBN were evaluated using 10-fold cross-validation,
586 running each train-test pair ten times, and calculating the mean classification accuracy (number of
587 sequences/sets of sequences correctly classified divided by total number of sequences/sets of
588 sequences). The training and test sets all consisted of equal numbers of DPC related and control
589 sequences, and running the DBN with shuffled class labels returned ~50% accuracy. The network
590 diagram in **Figure 7A** was created using the LaTeX TikZ Bayes package
591 (https://github.com/jluttine/tikz-bayesnet).

592

Conflict of Interest

594 The authors declare that this study received funding from Unilever PLC. GM is an employee of
595 Unilever PLC. Apart from GM's contribution (see author contributions) the funder was not involved in
596 the study design, collection, analysis, and interpretation of data, the writing of this article or the
597 decision to submit it for publication.

Funding

601 **Data availability.** All DNA sequences have been submitted to the Short Read Archive under
602 identifier **PRJNA592875** .

Supplementary file legends

604 **Supplementary File 1 Unique and total TCR numbers for each TCRseq sample.** '_TRA' are the
605 TCR alpha chain samples, and '_TRB' the beta chain samples.

Supplementary File 2 Repeated exposure to DPC does not alter the global structure of the peripheral blood TCR repertoire. (A) The Shannon diversity index of the healthy volunteers (n=14 samples from five individuals), pre-sensitization (n=25) and post-sensitization (n=58; from all three time points) TCR repertoire samples. All samples were randomly subsampled to the minimum sample size (20,172 alpha TCRs), and the Shannon diversity index of the subsample was then calculated. Each sample is represented by a dot. The box plots show the median, and lower and upper quartiles of each group. Differences in the distribution of the three groups were tested using Kruskal-Wallis rank sum test and were non-significant (p=0.7658). **(B)** The Gini inequality coefficient of the healthy volunteers, pre-sensitization and post-sensitization alpha chain TCR repertoire samples, subsampled as in (B). Differences in the distribution of the three groups were tested using a Kruskal-Wallis rank sum test and were non-significant (p=0.9062). **(C)** The number of alpha TCRs that appear with frequency of 1/1000 or higher in each sample (termed 'abundant TCRs'), for the healthy volunteers, pre-sensitization and post-sensitization samples, subsampled as in (A) and (B). A Kruskal-Wallis rank sum test revealed no statistical difference between the groups (p=0.9256). **(D)-(F)** The alpha chains of the sensitized samples were separated according to time point: PT1 (n=23), PT2 (n=18) and PT3 (n=17). The Shannon diversity index (D), the Gini coefficient (E) and the number of abundant clones (F) of these subsamples were calculated. Kruskal-Wallis rank sum tests were used to compare between the three groups in each case. All tests showed no statistically significant difference, with p=0.9608, p=0.9281 and p=0.8681 respectively.

Supplementary File 3 Sensitization with DPC induces a transient expansion in the frequency of a small subset of the TCR repertoire. (A) The abundance distribution of TCRs at PS and PT1. All samples were subsampled to the same number of TCRs (28,000). Each unique TCR is represented by a dot, and the axes represent the number of times it is observed in the PS (x axis) and PT1 (y axis) sample of the same individual, and equally spaced time points for the healthy volunteers. The pink dots identify a population of TCRs absent in the PS sample and expanded (abundance ≥ 8) in the PT1 sample. The blue dots identify a population of TCRs absent in the PT1 sample and expanded (≥ 8) in the PS sample. The numbers indicate the percentage of PT1 expanded TCRs (pink) and PS expanded TCRs (blue). **(B)** The correlation between the percentage of PT1 expanded alpha chain TCRs (x-axis) and the percentage of PT1 expanded beta chain TCRs (y-axis) for each individual (n=22), subsampled as in (A). Spearman's Rho=0.85, p<0.0001. The line x=y is shown.

Supplementary File 4 Dynamic changes in TCR frequency following sensitisation. (A) The abundances of the PT1 expanded (threshold ≥ 8) alpha TCRs at the four time points: PS, PT1, PT2, PT3. Each panel is a different patient (n=10). **(B)** The abundances of the PT2 expanded (threshold ≥ 8) alpha TCRs at the four time points: PS, PT1, PT2, PT3. Each panel is a different patient (n=10). **(C)** Equivalent time points (0 weeks, 2 weeks and 6 weeks) for four healthy volunteers for whom we had all three times points. Top row is PT1 expanded alpha TCRs; bottom row is PT2 expanded alpha TCRs. The fourth volunteer had no PT1 expanded alpha TCRs. The fifth volunteer had no PT1 expanded alpha TCRs and no PT2 alpha sample.

Supplementary File 5 Sequence alignment of the CDR3 sequences from the largest cluster of TCR alpha PT1 expanded CDR3s. The CDR3s of the largest cluster of PT1 expanded CDR3 beta sequences (see **Figure 6D** and **E**) were aligned using the MUSCLE alignment algorithm in Aliview (https://ormbunkar.se/aliview/).

Source data files

649 **Source data file 1. Table of expanded T cell receptors.** The list of T cell receptors which is used
650 to generate the DBN illustrated in Fig 7. Each row contains a unique combination of CDR3
651 sequence, V gene and J gene annotation.

652 **Source data file 2. Table of control T cell receptors.** The list of T cell receptors which is used as
653 the control set to generate the DBN illustrated in Fig 7. Each row contains a unique combination of
654 CDR3 sequence, V gene and J gene annotation.

655

656 **References**

657 Appay V, van Lier RAW, Sallusto F, Roederer M. 2008. Phenotype and function of human T
658   lymphocyte subsets: Consensus and issues. *Cytom Part A* **73A**:975–983.
659   doi:10.1002/cyto.a.20643

660 Ashworth J, Tuyp E, Mackie RM. 1989. Allergic and irritant contact dermatitis compared in the
661   treatment of alopecia totalis and universalis. A comparison of the value of topical
662   diphencyprone and tretinoin gel. *Br J Dermatol* **120**:397–401.

663 Buckley DA, Keane FM, Munn SE, Fuller LC, Higgins EM, Du Vivier AW. 1999. Recalcitrant viral
664   warts treated by diphencyprone immunotherapy. *Br J Dermatol* **141**:292–6.

665 Csardi G, Nepusz T. 2006. The igraph software package for complex network research. *InterJournal*
666   **Complex Sy**:1695.

667 Dagum P, Galper A, Horvitz E. 1992. Dynamic Network Models for Forecasting. *Uncertain Artif*
668   *Intell* 41–48. doi:10.1016/B978-1-4832-8287-9.50010-4

669 Dash P, Fiore-Gartland AJ, Hertz T, Wang GC, Sharma S, Souquette A, Crawford JC, Clemens EB,
670   Nguyen THO, Kedzierska K, La Gruta NL, Bradley P, Thomas PG. 2017. Quantifiable
671   predictive features define epitope-specific T cell receptor repertoires. *Nature* **547**:89–93.
672   doi:10.1038/nature22383

673 Davis MM, McHeyzer-Williams M, Chien YH. 1995. T-cell receptor V-region usage and antigen
674   specificity. The cytochrome c model system. *Ann N Y Acad Sci* **756**:1–11.

675 DeWitt WS, Emerson RO, Lindau P, Vignali M, Snyder TM, Desmarais C, Sanders C, Utsugi H,
676   Warren EH, McElrath J, Makar KW, Wald A, Robins HS. 2015. Dynamics of the cytotoxic T
677   cell response to a model of acute viral infection. *J Virol* **89**:4517–26. doi:10.1128/JVI.03474-14

678 Glanville J, Huang H, Nau A, Hatton O, Wagar LE, Rubelt F, Ji X, Han A, Krams SM, Pettus C,
679   Haas N, Arlehamn CSL, Sette A, Boyd SD, Scriba TJ, Martinez OM, Davis MM. 2017.
680   Identifying specificity groups in the T cell receptor repertoire. *Nature* **547**:94–98.
681   doi:10.1038/nature22976

682 Karanovic S, Harries M, Kaur MR. 2018. Diphenylcyclopropenone for alopecia areata: a U.K.
683   survey. *Br J Dermatol*. doi:10.1111/bjd.16489

684 Karatzoglou A, Smola A, Hornik K, Zeileis A. 2004. **kernlab** - An *S4* Package for Kernel Methods
685   in *R*. *J Stat Softw* **11**:1–20. doi:10.18637/jss.v011.i09

686 Kimber I, Maxwell G, Gilmour N, Dearman RJ, Friedmann PS, Martin SF. 2012. Allergic contact
687   dermatitis: a commentary on the relationship between T lymphocytes and skin sensitising
688   potency. *Toxicology* **291**:18–24. doi:10.1016/j.tox.2011.11.007

689 Larsson A. 2014. AliView: a fast and lightweight alignment viewer and editor for large datasets.
690   *Bioinformatics* **30**:3276–8. doi:10.1093/bioinformatics/btu531

691 Lee S, Kim BJ, Lee Y Bin, Lee W-S. 2018. Hair Regrowth Outcomes of Contact Immunotherapy for
692   Patients With Alopecia Areata: A Systematic Review and Meta-analysis. *JAMA dermatology*
693   **154**:1145–1151. doi:10.1001/jamadermatol.2018.2312

694 Moos S, Johansen P, Waeckerle-Men Y, Mohanan D, Senti G, Häffner A, Kündig TM. 2012. The
695   contact sensitizer diphenylcyclopropenone has adjuvant properties in mice and potential
696   application in epicutaneous immunotherapy. *Allergy* **67**:638–646. doi:10.1111/j.1398-
697   9995.2012.02802.x

698 Mose K.F., Andersen F, Skov L, Røpke MA, Litman T, Friedmann PS, Andersen KE. 2017.
699   Repeated monthly epicutaneous challenges with diphenylcyclopropenone result in a clinically
700   reproducible level of contact allergy in *de novo* sensitized individuals. *Br J Dermatol* **176**:1095–
701   1097. doi:10.1111/bjd.14949

702 Mose Kristian F, Burton M, Thomassen M, Andersen F, Kruse TA, Tan Q, Skov L, Røpke MA,
703   Litman T, Clemmensen O, Kristensen BW, Friedmann PS, Andersen KE. 2017. The gene
704   expression and immunohistochemical time-course of diphenylcyclopropenone-induced contact
705   allergy in healthy humans following repeated epicutaneous challenges. *Exp Dermatol* **26**:926–
706   933. doi:10.1111/exd.13345

707 Murphy K, Mian S. 1999. Modelling Gene Expression Data Using Dynamic Bayesian Networks.
708   *Tech Report, Univ California*.

709 Murphy KP. 2001. The Bayes Net Toolbox for MATLAB. *Comput Sci Stat* **33**:2001.

710 Murphy KP, Russell SJ. 2002. Dynamic bayesian networks: representation, inference and learning.

711 Oakes T, Heather JM, Best K, Byng-Maddick R, Husovsky C, Ismail M, Joshi K, Maxwell G,
712   Noursadeghi M, Riddell N, Ruehl T, Turner CT, Uddin I, Chain B. 2017a. Quantitative
713   Characterization of the T Cell Receptor Repertoire of Naïve and Memory Subsets Using an
714   Integrated Experimental and Computational Pipeline Which Is Robust, Economical, and
715   Versatile. *Front Immunol* **8**. doi:10.3389/FIMMU.2017.01267

716 Oakes T, Popple AL, Williams J, Best K, Heather JM, Ismail M, Maxwell G, Gellatly N, Dearman
717   RJ, Kimber I, Chain B. 2017b. The T Cell Response to the Contact Sensitizer
718   Paraphenylenediamine Is Characterized by a Polyclonal Diverse Repertoire of Antigen-Specific
719   Receptors. *Front Immunol* **8**:162. doi:10.3389/fimmu.2017.00162

720 Pearl J. 1988. Probabilistic reasoning in intelligent systems : networks of plausible inference.
721   Elsevier. doi:https://doi.org/10.1016/C2009-0-27609-4

722 Pogorelyy M V, Minervina AA, Shugay M, Chudakov DM, Lebedev YB, Mora T, Walczak AM.
723   2019. Detecting T cell receptors involved in immune responses from single repertoire snapshots.

724   *PLoS Biol* **17**:e3000314. doi:10.1371/journal.pbio.3000314

725   Pogorelyy M V, Minervina AA, Touzel MP, Sycheva AL, Komech EA, Kovalenko EI, Karganova
726   GG, Egorov ES, Komkov AY, Chudakov DM, Mamedov IZ, Mora T, Walczak AM, Lebedev
727   YB. 2018. Precise tracking of vaccine-responding T cell clones reveals convergent and
728   personalized response in identical twins. *Proc Natl Acad Sci U S A* **115**:12704–12709.
729   doi:10.1073/pnas.1809642115

730   Read T, Webber S, Tan J, Wagels M, Schaider H, Soyer HP, Smithers BM. 2017.
731   Diphenylcyclopropenone for the treatment of cutaneous in-transit melanoma metastases - results
732   of a prospective, non-randomized, single-centre study. *J Eur Acad Dermatology Venereol*
733   **31**:2030–2037. doi:10.1111/jdv.14422

734   Shawe-Taylor J, Cristianini N. 2004. Kernel methods for pattern analysis. Cambridge university
735   press.

736   Stute J, Hausen BM, Schulz KH. 1981. [Diphenylcyclopropenone - a new strong contact sensitizer
737   (author's transl)]. *Derm Beruf Umwelt* **29**:12–4.

738   Sun Y, Best K, Cinelli M, Heather JM, Reich-Zeliger S, Shifrut E, Friedman N, Shawe-Taylor J,
739   Chain B. 2017. Specificity, privacy, and degeneracy in the CD4 T cell receptor repertoire
740   following immunization. *Front Immunol* **8**. doi:10.3389/fimmu.2017.00430

741   Thomas N, Best K, Cinelli M, Reich-Zeliger S, Gal H, Shifrut E, Madi A, Friedman N, Shawe-
742   Taylor J, Chain B. 2014. Tracking global changes induced in the CD4 T-cell receptor repertoire
743   by immunization with a complex antigen using short stretches of CDR3 protein sequence.
744   *Bioinformatics* **30**. doi:10.1093/bioinformatics/btu523

745   Uddin I, Joshi K, Oakes T, Heather JM, Swanton C, Chain B. 2019. An economical, quantitative, and
746   robust protocol for high-throughput T cell receptor sequencing from tumor or blood.Methods in
747   Molecular Biology. pp. 15–42. doi:10.1007/978-1-4939-8885-3_2

748   Wilkerson MG, Connor TH, Henkin J, Wilkin JK, Matney TS. 1987. Assessment of
749   diphenylcyclopropenone for photochemically induced mutagenicity in the Ames assay. *J Am*
750   *Acad Dermatol* **17**:606–11.

751   Yao X-Q, Zhu H, She Z-S. 2008. A dynamic Bayesian network approach to protein secondary
752   structure prediction. *BMC Bioinformatics* **9**:49. doi:10.1186/1471-2105-9-49

753